THE JOURNAL OF PHYSICAL CHEMISTRY C

Article

pubs.acs.org/JPCC

Modulation of Fluorescence Resonance Energy Transfer Efficiency for White Light Emission from a Series of Stilbene-Perylene Based Donor–Acceptor Pair

Dibakar Kumar Maiti,[†] Rameswar Bhattacharjee,[‡] Ayan Datta,[‡] and Arindam Banerjee*[,†]

[†]Department of Biological Chemistry, and [‡]Department of Spectroscopy, Indian Association for the Cultivation of Science, Jadavpur, Kolkata, 700032 India

Supporting Information

ABSTRACT: The discovery of white light emitting materials is a highly emerging field. Stilbene moiety containing three donor molecules and perylene moiety containing three acceptor molecules have been selected for various donor–acceptor sets in Förster resonance energy transfer (FRET). An attempt has been made to correlate energy transfer efficiency with the emission of white light. It has been found that generally good energy transfer efficiency leads to significant white light emission, while poor energy transfer efficiency shows no significant emission of white light. Results of computational studies also match well with experimental results for measuring energy transfer in FRET. Results of this study are promising for making new white light emitting materials in the future based on the proper selection of donor–acceptor pair in FRET.

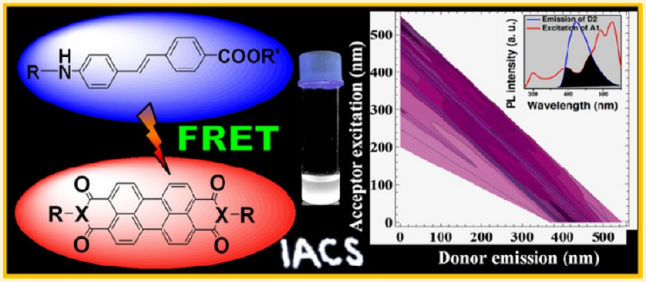

INTRODUCTION

In recent years, light emitting devices have accounted for about 20% of worldwide energy consumption.[1−3] So, the development of efficient light sources is becoming increasingly important. White light emission has widespread applications in different devices and displays.[4−6] Generally white light emission is obtainable by mixing different combinations of luminophores either through covalent linkage or by using self-assembly.[7−9] However, the major challenge is to maintain the critical balance between different luminophores and to carefully control the energy transfer between the donor–acceptor pair for multicomponent white light emitting material. A single molecule luminophore that exhibits white light emission covering a broad range of emission from blue to red is also reported in the literature.[10−12] There are several examples of white light emitting materials involving organic–inorganic hybrid,[13,14] organic-π conjugated system based on donor–acceptor molecules,[15] polymers,[16−18] metal complexes,[19−23] micro and nanomaterials,[24−26] and others.[27−32] There are also a few examples of solid state white light emitting substances and solvent free white light emitting organic materials.[33,34] However, solution processable white light emitting substance is also important as it can be soaked on a solid surface or it can be coated over a surface to generate white light emission.

The judicious choice of a donor–acceptor pair in generating white light emission still remains to be a challenging task. There are some examples of two component white light emitting systems by utilizing a Förster resonance energy transfer (FRET) process.[35,36] However, discovering a new series of donor–acceptor sets in FRET leading to the white light emission is still a challenging task. So, careful selection of organic donor and acceptor molecules and to control the energy transfer between them to produce processable white light emitting substance is needed indeed.

FRET[37,38] is a very good and well established technique to measure the distance between the donor and acceptor molecules and this has been used as a spectroscopic ruler.[39,40] It has various applications in biological sciences,[41,42] sensors,[43,44] material sciences,[45−47] and chemical sciences.[48−52] An attempt can also be made to utilize this FRET technique to measure the energy transfer efficiency and to correlate this efficiency for generating white light emission in a two or more component system. In other way, it can be stated that energy transfer efficiency can be used as an indicator for white light emission. In this study, we want to address the question whether white light emission is predictable depending on the nature of energy transfer efficiency, whether it is poor or good.

In this study, we present the participation of a series of stilbene moiety containing donor molecules and a series of perylene moiety containing acceptor molecules in FRET and the efficiency of the energy transfer in FRET is easily tunable by manipulating the structure of donor and acceptor molecules leading to the formation white light emitting materials. Computational studies have been aimed at explaining the energy transfer efficiency in FRET for different sets of a donor–acceptor pair. Good energy transfer efficiency leads to white light emission and poor energy transfer efficiency does not allow

Received: September 10, 2013
Revised: September 26, 2013
Published: September 30, 2013

 © 2013 American Chemical Society dx.doi.org/10.1021/jp409042p | J. Phys. Chem. C 2013, 117, 23178−23189

any emission of white light with only one exception out of nine donor–acceptor pair. Moreover, most of these donor–acceptor sets (seven out of nine) under suitable conditions emit white light.

RESULTS AND DISCUSSION

Synthesis. The synthetic method for making stilbene moiety containing donors (**D2** and **D3**; Figure 1) were reported by us earlier.[53] **D2** has been synthesized by palladium mediated coupling according to scheme 1.

All peptides and amino acid derivatives were synthesized in solution phase. Peptides were synthesized from amino acids by coupling using *N*,*N*-dicyclohexylcarbodiimide (DCC; Scheme 2).

Another donor **D3** was synthesized according to scheme 3 by coupling between **7** and **3**. Perylene containing acceptor molecule **A1** was synthesized and characterized according to the literature procedure.[54,55] Perylenediimide (PDI) containing acceptor molecules **A2** and **A3** were synthesized by coupling with appropriate amino acid or peptide derivatives (Scheme 4). These compounds were well characterized by ^{1}H NMR spectroscopy and high resolution mass spectroscopy (HRMS), and these pure compounds were used for all studies.

Our earlier studies have shown stilbene-perylenediimide can be used as a good donor–acceptor in FRET for generating white light.[31] We are trying to make an effort to correlate the energy transfer efficiency with the emission of white light. Stilbene based three donor molecules and perylene based three acceptor molecules have been chosen for FRET studies. A total of nine donor–acceptor pairs have been used for Förster resonance energy transfer. Seven out of nine combinations have produced white light. The main aim of the study is to look for a prediction method for white light emission based on donor–acceptor energy transfer efficiency in FRET.

General Spectroscopic Characterization. *UV–vis Spectroscopy.* UV–vis spectroscopic studies were carried out to probe the absorbance patterns of these donors and acceptors. In all UV–vis experiments, chlorobenzene was used as the solvent. The individual UV–vis absorption spectrum of **D1** shows an absorption band centered at 307 nm (Figure 2). Molecules **D2** and **D3** show absorption bands at 345 and 344 nm, respectively, in chlorobenzene solution. Solutions of these three donor molecules (**D1**, **D2**, and **D3**) emit blue fluorescence upon the exposure of the UV lamp at 365 nm. The substitution of the 4,4′-hydrogens in stilbene (**D1**) by an amino and a carboxylic group causes a red shift (about 50 nm) of the absorption spectrum compared to the **D1** molecule in chlorobenzene solution (Figure 2).

UV–vis spectra of all acceptor molecules are shown in Figure 2. The UV–vis spectrum of the molecule **A1** shows

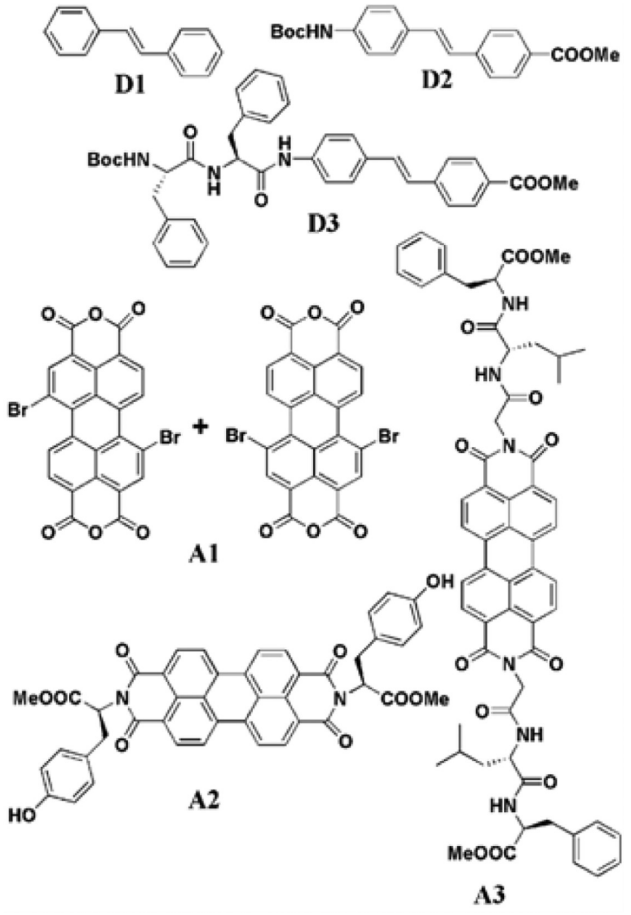

Figure 1. Chemical structures of the donor (**D1**, **D2**, and **D3**) and the acceptor (**A1**, **A2**, and **A3**) molecules.

Scheme 1. Synthesis of Donor D2

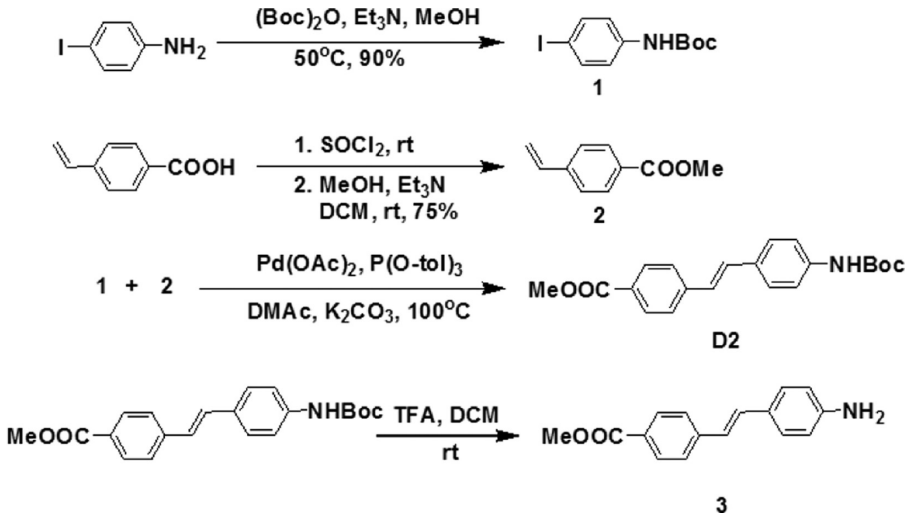

dx.doi.org/10.1021/jp409042p | J. Phys. Chem. C 2013, 117, 23178–23189

Scheme 2. Synthesis of Peptides and Amino Acid Derivatives

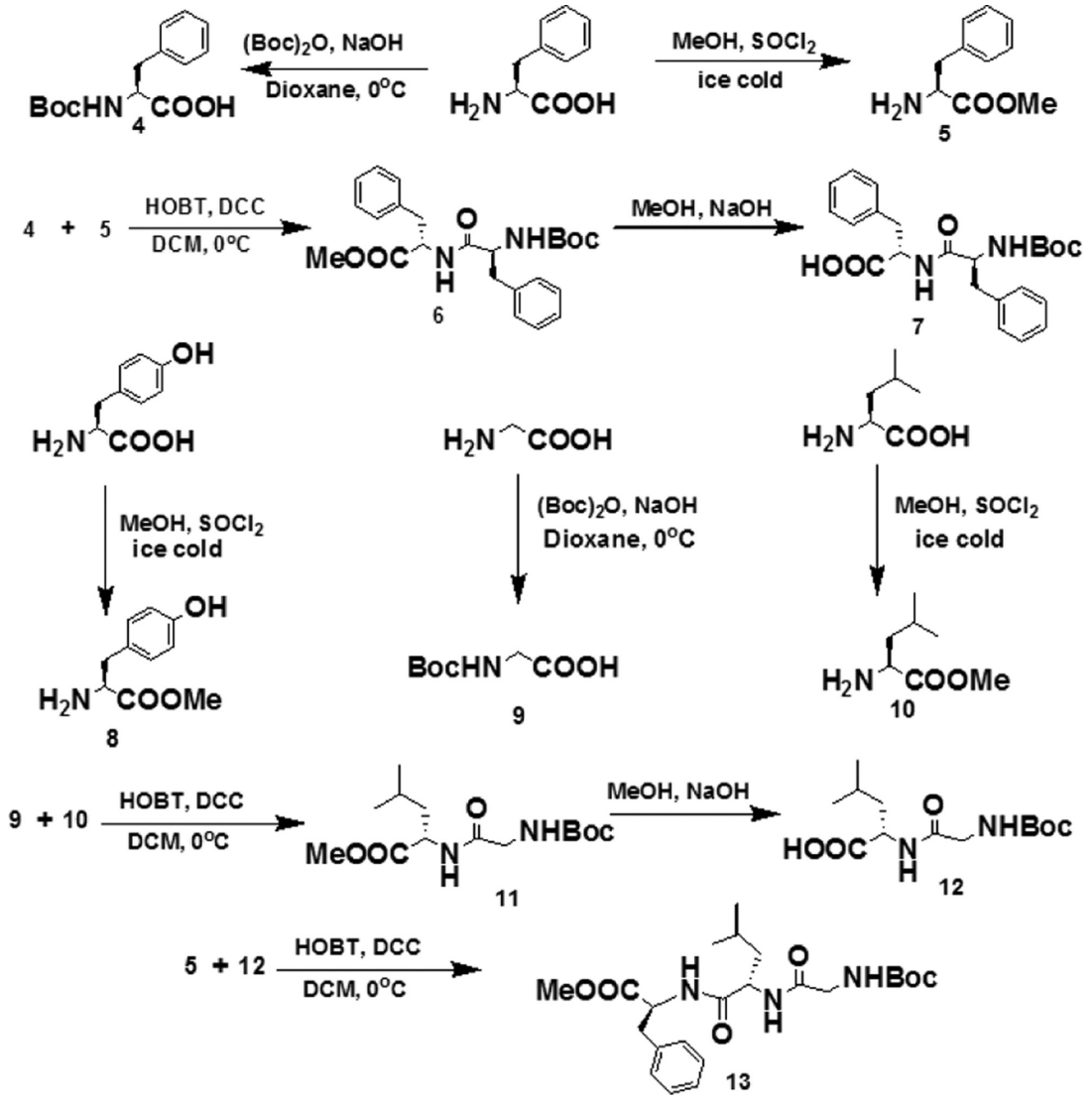

several peaks at 525, 490, and 459 nm, out of which the peak at 525 nm has the highest intensity (Figure 2).

Chlorobenzene solution of the molecule **A2** also shows a similar pattern in its absorption spectrum. There are three peaks at 532, 495, and 464 nm and the peak at 532 nm is the major peak. The acceptor **A3** shows three absorption bands in its UV−vis absorption spectrum (Figure 2). They are at 529, 490, and 460 nm, out of which the peak at 529 nm is the major absorption peak. All of these three acceptors (**A1, A2** ,and **A3**) in chlorobenzene solution emit orange fluorescence upon the exposure of the UV lamp at 365 nm.

Fluorescence Spectroscopy. Fluorescence spectroscopic studies of all donors and acceptors were carried out in chlorobenzene solvent to examine their respective fluorescence excitation and emission spectra. The individual fluorescence spectroscopic study of **D1** shows an emission peak at 358 nm with a hump at 374 nm (Figure 3). **D1** shows a strong fluorescence excitation peak at 331 nm with a hump at 296 nm, whereas the stilbene based compound **D2** shows only one peak in its fluorescence emission spectrum at 423 nm. The fluorescence excitation spectrum of **D2** shows a peak at 367 nm with a very broad hump at 321 nm (Figure 3). The donor **D3** shows its fluorescence excitation at 342 nm and emission at 421 nm in its fluorescence excitation and emission spectra, respectively (Figure 3). All of these results indicate that stilbene based donor molecules **D1**, **D2**, and **D3** are blue emitters. Moreover, the substitution of 4,4′-hydrogens of stilbene (**D1**) by an amino group and a carboxylic group results in the red shift of the fluorescence excitation and emission peaks.

The fluorescence spectroscopic study of the bromo derivative of perylene bisanhydride **A1** shows the characteristic excitation and emission peaks of the perylene core. It shows two emission peaks at 550 and 590 nm upon the excitation at 528 nm. The peak at 550 nm has the higher intensity (Figure 3). This acceptor **A1** has a very interesting fluorescence excitation spectrum pattern. It shows two sharp peaks at 528 and 492 nm with a hump at 461 nm. The peak centered at 528 nm is the major fluorescence excitation peak. Apart from these peaks, there is also a broad weak fluorescence excitation band within 300 to 450 nm, and this is also a characteristic excitation band of the perylene core. The acceptor **A2** shows two sharp emission peaks at 540 and 583 nm with a hump at 634 nm upon the excitation at 534 nm (Figure 3). The peak at 540 nm is the major peak with the highest intensity. **A2** shows two

dx.doi.org/10.1021/jp409042p | J. Phys. Chem. C 2013, 117, 23178−23189

Scheme 3. Synthesis Scheme of Donor D3

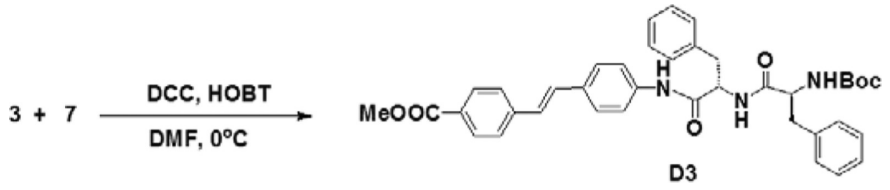

Scheme 4. Synthesis Scheme of Acceptors A1, A2, and A3

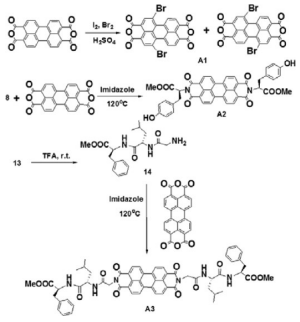

major fluorescence excitation peaks at 534 and 495 nm with a hump at 464 nm. In this case, a weak broad fluorescence excitation is also observable from 300 to 400 nm. The acceptor **A3** exhibits two major emission peaks at 538 and 583 nm with a broad hump at 635 nm (Figure 3). The fluorescence excitation spectrum shows two major peaks at 529 and 490 nm with a small hump at 460 nm. **A3** also has a weak fluorescence excitation within 300 to 400 nm. The above-mentioned fluorescence spectroscopic study suggests that these three acceptors **A1**, **A2**, and **A3** are orange fluorescence emitting materials in chlorobenzene solution. This is also supported by the observation of bright orange fluorescence obtained for all these three acceptors (**A1**, **A2**, and **A3**) upon the exposure of the UV lamp at 365 nm (Figure 2). Quantum yields of each of these compounds are determined. These values are as follows: **D1**, 5.43%; **D2**, 5.34%; **D3**, 6.72%; **A1**, 39.60%; **A2**, 32.17%; and **A3**, 33.06%.

Energy Transfer and White Light Processing Studies. *UV–vis Spectroscopy.* UV–vis spectroscopic studies of all combinations of these donors and acceptors were carried out to examine spectral characteristic features of each of these donor–acceptor pair. Each combination of donor–acceptor pair remarkably shows a wide range of absorption in their respective UV–vis spectrum. In case of two donor–acceptor pair **D1-A2** and **D1-A3**, no white light emission is obtained upon the exposure of UV lamp (365 nm). Interestingly, for all other donor–acceptor pair (**D1-A2**, **D2-A1**, **D2-A2**, **D2-A3**, **D3-A1**, **D3-A2**, and **D3-A3**), the respective absorption spectrum shows a wide range of absorption from 350 to 600 nm (Figure 4). A certain ratio of donor and acceptor component in each of these seven combinations emits white light in chlorobenzene solution upon the exposure to a UV-lamp of 365 nm. UV–vis spectra of all of these white light emitting solutions are presented in Figure 4.

Fluorescence Spectroscopy. The fluorescence spectroscopy is a very informative tool to demonstrate the energy transfer between a donor–acceptor pair (Figure 5). Efficient fluorescence resonance energy transfer (FRET) occurred for six donor–acceptor pair (**D2-A1**, **D2-A2**, **D2-A3**, **D3-A1**, **D3-A2**, and **D3-A3**) and for other three pair (**D1-A1**, **D1-A2**m and **D1-A3**) no fluorescence energy transfer was taken place. Interestingly, only a certain ratio of donor and acceptor exhibits a white light emission for each of these six pair. In this study, the **D2-A1** pair is discussed in details as a representative example. The chlorobenzene solution of **D2** (2.8×10^{-5} M) shows the fluorescence emission peak at 423 nm upon excitation at its fluorescence excitation wavelength 367 nm. The gradual addition of **A1** (7×10^{-6} to 4.2×10^{-5} M) causes a decrease in intensity of the peak at 423 nm (upon excitation at 367 nm) and peaks at 550 and 590 nm are steadily increased in intensity. Thus, the fluorescence emission peak intensity at 423 nm decreases due to the fluorescence resonance energy transfer from **D2** to **A1**. This type of energy transfer observation demonstrates that **D2** and **D3** act as donor and **A1**, **A2**, **A3** act as acceptor. For each combination of donor–acceptor pair (**D2-A1**, **D2-A2**, **D2-A3**, **D3-A1**, **D3-A2**, and **D3-A3**), the gradual addition of the acceptor to the donor is associated with a steady decrease in intensity of the donor's fluorescence emission peak with the steady increase of the intensity of acceptor's emission peak (Figure 5). It is interesting to observe that combinations with **D1** is not successful for energy transfer due to the poor overlaps of the donor's emission spectrum and acceptor's excitation spectrum (Figure 5). The substitution of 4,4′-hydrogens in stilbene (**D1**) by an amino group and a carboxylic group in **D2** and **D3** results

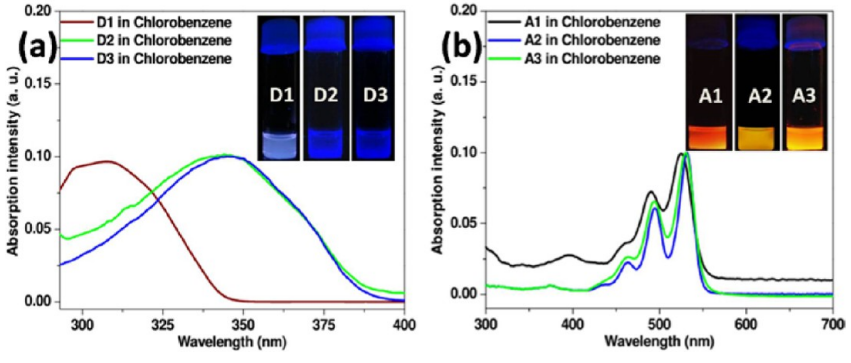

Figure 2. UV–vis absorption spectra of donors **D1** (a), **D2** (b), and **D3** (c) and acceptors **A1** (d), **A2** (e), and **A3** (f) in chlorobenzene solution.

dx.doi.org/10.1021/jp409042p | J. Phys. Chem. C 2013, 117, 23178–23189

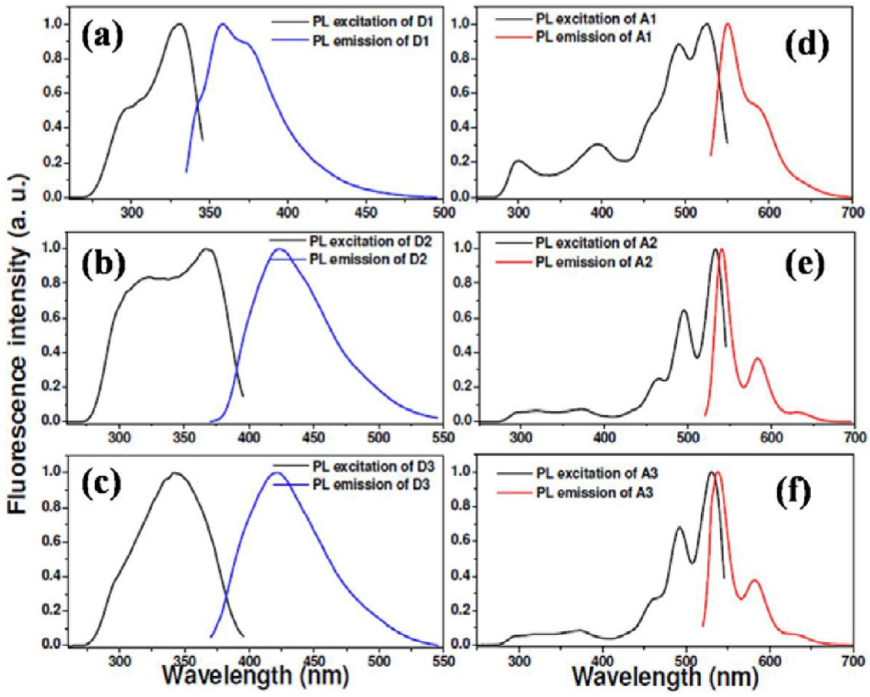

Figure 3. Fluorescence excitation and emission spectra of donors **D1** (a), **D2** (b), and **D3** (c) and acceptors **A1** (d), **A2** (e), and **A3** (f) in chlorobenzene solution. Excitation and emission spectra are indicated within corresponding figures.

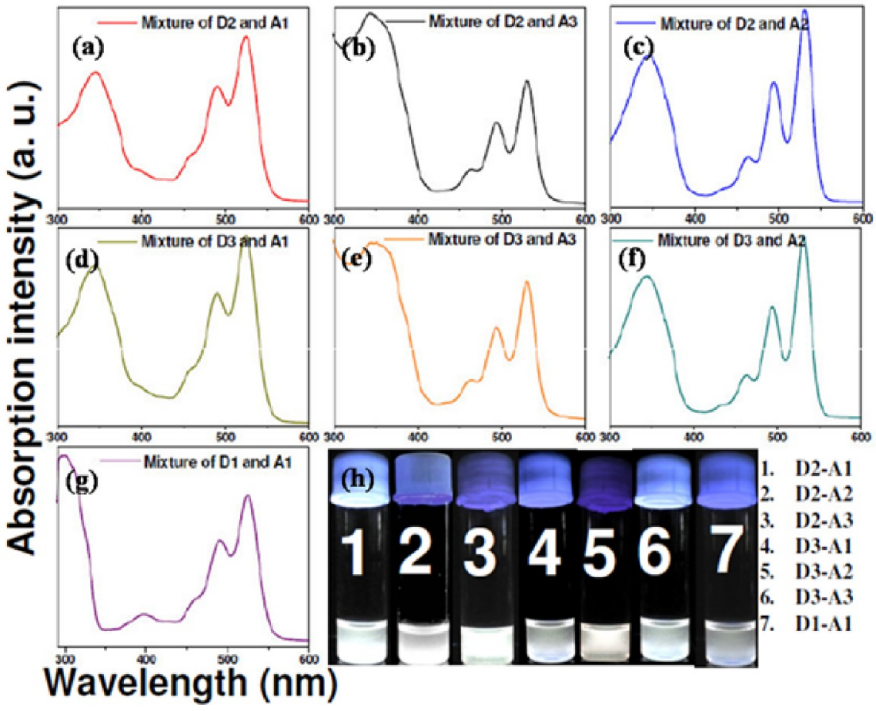

Figure 4. UV−vis absorption spectra of white light emitting solutions of different pair of donors and acceptors: **D2-A1** (a), **D2-A3** (b), **D2-A2** (c), **D3-A1** (d), **D3-A3** (e), **D3-A2** (f), and **D1-A1** (g). (h) White light emitting solutions exposed to the UV lamp at 365 nm.

in a red shift of the corresponding fluorescence emission peak of donors **D2** and **D3**. This is actually responsible for the better overlap between the fluorescence excitation peaks of the acceptor (**A1**, **A2**, and **A3**) molecules with each of these donor (**D2** and **D3**) molecules' emission. So, it can be stated that efficient energy transfers occur involving those donor−acceptor pair, which contains either **D2** or **D3** as the donor molecule.

Comparison between the UV−vis Spectra and Fluorescence Excitation Spectra. Comparison between the UV−vis absorption spectra and fluorescence excitation spectra for three donor and acceptor containing solutions were performed. All these experiments were carried out with a common acceptor molecule **A2** and three different donor molecules (**D1**, **D2**, and **D3**). The UV−vis spectrum

dx.doi.org/10.1021/jp409042p | J. Phys. Chem. C 2013, 117, 23178−23189

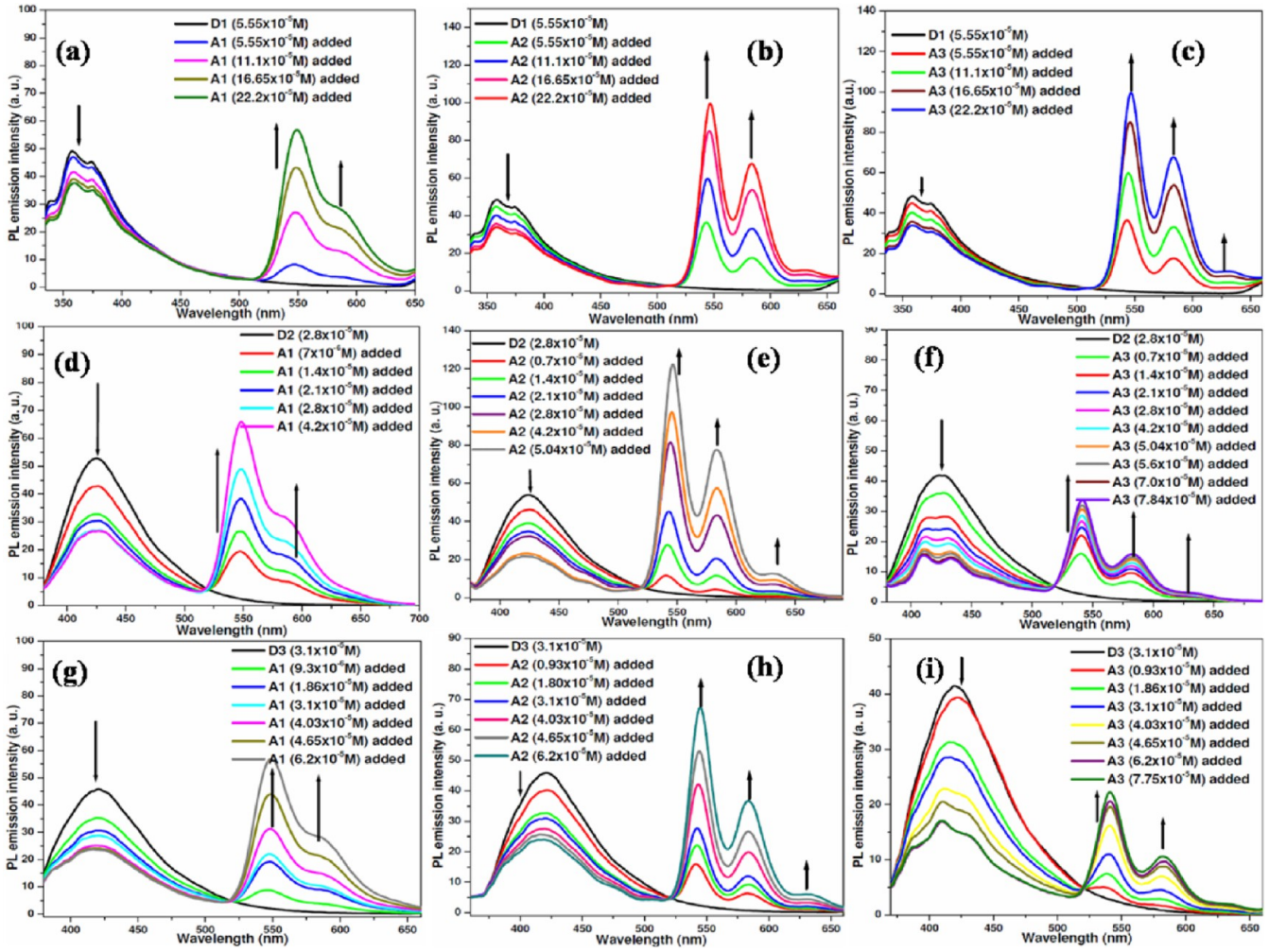

Figure 5. Changes in fluorescence spectra of donors upon the gradual addition of acceptor to the respective donors: **D1-A1** (a), **D1-A2** (b), **D1-A3** (c), **D2-A1** (d), **D2-A2** (e), **D2-A3** (f), **D3-A1** (g), **D3-A2** (h), and **D3-A3** (i). Added concentration of the corresponding acceptors are indicated in respective figures.

of **D1-A2** pair contains all peaks corresponding to **D1** as well as **A2**.

However, the fluorescence excitation of the same solution exhibits only those peaks which are corresponding to the acceptor's (**A2**) excitation wavelength (Figure 6) for emission at 547 nm. This indicates that practically there is no energy transfer between the **D1-A2** pair. Interestingly, for the donor−acceptor pair **D2-A2** the fluorescence excitation spectrum shows the major peak at 370 nm corresponding to the excitation wavelength of the donor **D2**. This convincingly suggests that FRET is occurring between **D2** and **A2** leading to the significant contribution of the donor **D2** in the emission spectrum of acceptor **A2** at 540 nm. Similar observation is also found for the **D3-A2** donor−acceptor pair. These observations clearly suggest that significant energy transfer is occurring involving donors **D2** or **D3** and **A2**, whereas no energy transfer is apparent involving the donor **D1** and acceptor **A2**. To explain these phenomenon the overlap integrals, Förster distances and maximum energy transfer efficiencies were calculated experimentally for each donor−acceptor pair.

Overlap Integrals, Förster Distances, and Maximum Energy Transfer Efficiency. There are overlaps between the fluorescence excitation spectrum of acceptor molecule and fluorescence emission spectrum of the donor molecule (Figure 7), and this is very important for the occurrence of a successful resonance energy transfer. The FRET parameters overlap integral (J), Förster distances (R_0), and intermolecular distances (r) are determined by using equations S1, S2 and S3 mentioned in the Supporting Information. The energy transfer efficiencies were determined by using the following equation:[37,38]

$$E = 1 - \frac{F_{DA}}{F_D} \quad (1)$$

In this case for each donor−acceptor the fluorescence emission spectrum of the donor and the fluorescence excitation spectrum of the acceptor were plotted in the same graph at normalized condition (Figure 7) and the overlap integrals were calculated. It is evident from figure 7 that the spectral overlaps are quite sufficient for the combinations **D2-A1**, **D2-A2**, **D2-A3**, **D3-A1**, **D3-A2**, and **D3-A3** that leads to the efficient energy transfer from donor to acceptor. However, spectral overlaps are not sufficient for **D1-A1**, **D1-A2**, and **D1-A3** pair leading no significant transfer to occur. Table 1 demonstrates the efficiency of energy transfer among each pair of donor and acceptor.

The energy transfer efficiency calculations from experimental values has confirmed that the efficiencies of energy transfer from donor to acceptor are decreasing with an increase in the

dx.doi.org/10.1021/jp409042p | J. Phys. Chem. C 2013, 117, 23178−23189

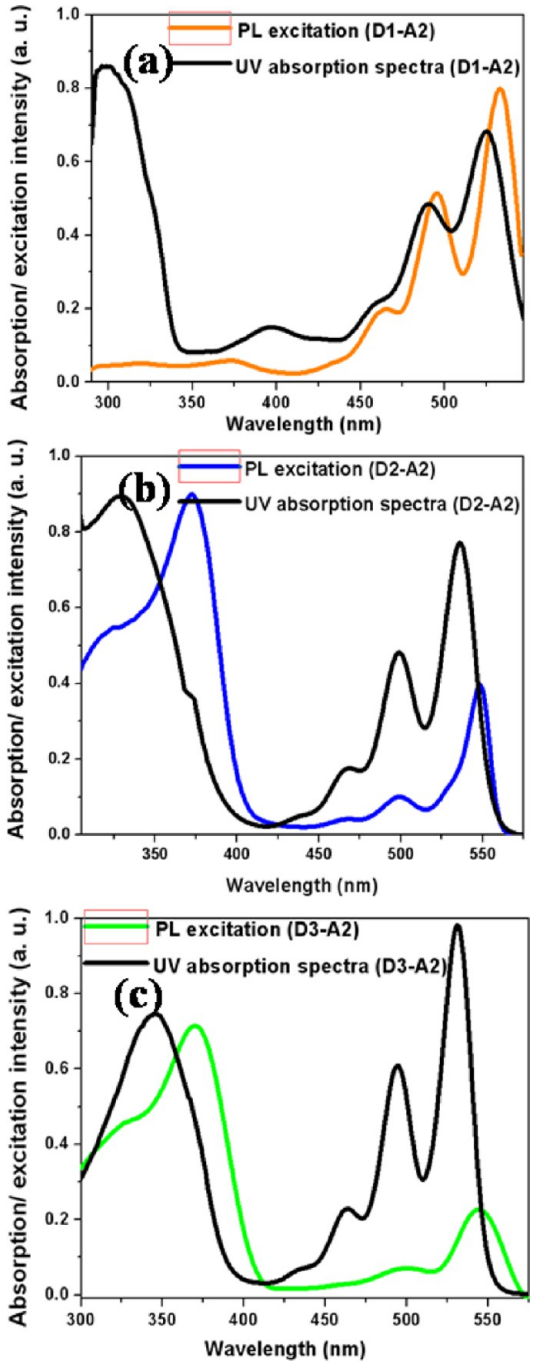

Figure 6. Comparison between PL excitation spectrum and UV−vis absorption spectrum of various donors with the acceptor **A2**: **D1-A2** (a), **D2-A2** (b), and **D3-A2** (c).

intermolecular distances (r) between the donor and acceptor molecule. Moreover, the plot of energy transfer efficiency versus intermolecular distance show the low RET between **D1** and other acceptors (**A1**, **A2**, and **A3**; Figure 8). This plot (Figure 8) is potentially important for measuring distance of 20−40 Å, that indicates the donor−acceptor set can be used as a spectroscopic ruler.

Time Correlated Single Photon Count (TCSPC) Study. Average fluorescence lifetimes were determined by performing the TCSPC experiments. In this study, chlorobenzene was also taken as the solvent to carry out all experiments. Only **D1**, **D2**, **A1**, and **A2** were examined for this purpose. For measuring the lifetime of **D1** and **D2**, samples were excited at 340 and 375 nm respectively nearer to their excitation wavelength. The average lifetime of **D1** and **D2** were 0.18 ns (recorded at 358 nm) and 0.21 ns (recorded at 423 nm) respectively. To measure the average fluorescence lifetime of acceptors the samples were excited at 440 nm and the emissions were recorded at 550 nm. The average lifetime of **A1** and **A2** are estimated to be 5.36 and 5.38 ns, respectively (Figure 9).

However, in presence of the acceptor the average fluorescence lifetimes of donors are changed. It is obtained from the data that the average fluorescence lifetime of the donor was decreased in presence of the acceptor (Figure 10).

Moreover, the energy transfer efficiencies for each combination were determined by using the following equation:[37,38]

$$E = 1 - \frac{\tau_{DA}}{\tau_{D}} \tag{2}$$

where E is the energy transfer efficiency, τ_{DA} is the donor's lifetime in presence of the acceptor, and τ_{D} is the donor's lifetime in absence of the acceptor.

The results are given in Table2.

It is evident from Table 2 that the donor−acceptor consisting of **D2** are very efficient for energy transfer, whereas the **D1** containing donor−acceptor pair are less efficient for the energy transfer. These results are matched quite well with the energy transfer efficiency data obtained by using integral area calculation method in eq 1.

Computational Insights. For a microscopic understanding of the mechanism of RET in our systems, DFT calculations were performed at the M06-2X/6-31+g(d,p) level of theory using the Gaussian 09 suite of programs.[56] The ability of the M06-2X functional to account for dispersion interactions in π-stacked systems has been well-established.[57−59] Time-dependent DFT (TDDFT) calculations were performed to model the emission and absorption process of the donor and acceptor by considering 20 excited states each. For making the calculations computationally tractable, −BOC and $-CH_3$ groups in **D2** were substituted by hydrogens, whereas perylenebisanhydride and perylenediimide were chosen as models for **A1** and **A2**, respectively. Table 3 shows the important electronic transitions for **D1**, **D2**, **A1**, and **A2** alongwith their emission/absorption wavelengths and oscillator strengths. For both absorption and emission, electronic transitions are composed of entirely HOMO → LUMO and LUMO → HOMO levels, respectively. Figure S11 shows the HOMO and LUMO plots for **D1**, **D2**, **A1**, and **A2**.

Figure 11 shows the donor emission and acceptor excitation profiles for the **D1-A1**, **D1-A2**, **D2-A1**, and **D2-A2** pair. From both the contour plots as well as the spectral plots, good overlap for the **D2−A1** and **D2−A2** pair are evident, whereas the overlap is poor for **D1-A1** and **D1-A2**. Agreement between the experimental and the theoretical plots are excellent which suggests that the TDDFT calculations on the model systems capture the essential excitation profile for our systems. A poor overlap of the donor emission and the acceptor absorption for the **D1-A1** and **D1-A2** pair explains their low resonance energy transfer (RET).

So, as to understand the local interactions between the "effective" FRET pair namely **D2-A1** and **D2-A2**, structures for the molecular dimers were optimized. As it is seen from Figure 12, donors and acceptors are arranged in an almost perfectly parallel π-stacked fashion where a possibility of intermolecular N−H···O hydrogen bonding is present. Hydrogen

dx.doi.org/10.1021/jp409042p | J. Phys. Chem. C 2013, 117, 23178−23189

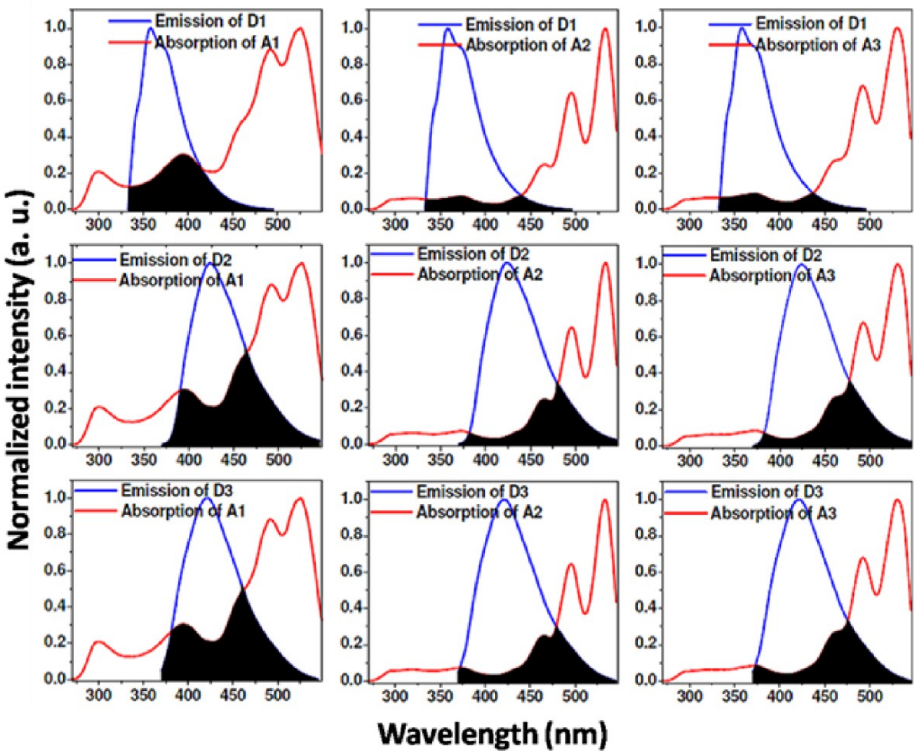

Figure 7. Overlaps between various emission spectra of donors and excitation spectra of acceptors.

Table 1. Energy Transfer Efficiency (E) and Förster Distance (R_0) Calculation Data for Each Pair of Donor and Acceptor[a]

donor	acceptor	$J(\lambda)$ in (M^{-1} cm^{-1} nm^4)	R_0 in Å	max E
D1	A1	1.36×10^{14}	20.74	0.18
D1	A2	3.27×10^{13}	16.36	0.27
D1	A3	3.64×10^{13}	16.65	0.27
D2	A1	4.42×10^{14}	25.16	0.48
D2	A2	2.99×10^{14}	23.57	0.60
D2	A3	2.60×10^{14}	23.04	0.65
D3	A1	6.24×10^{14}	27.71	0.44
D3	A2	1.23×10^{14}	21.14	0.46
D3	A3	2.21×10^{14}	23.32	0.59

[a] $\kappa^2 = 2/3$, $\eta = 1.5248$.

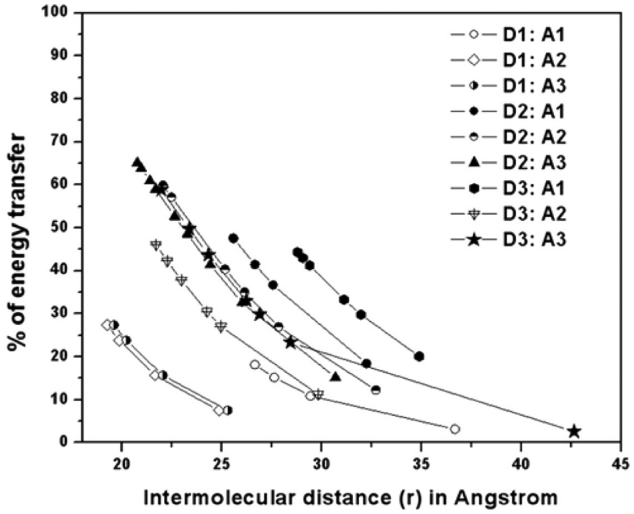

Figure 8. Energy transfer efficiency vs intermolecular distance plots for different donor−acceptor pairs.

bonding interaction between donor and acceptor molecules can play an important role in enhancing the efficiency of the FRET.[60−62] The average distance between the pair are ∼3.3 and 3.5 Å for **D2-A1** and **D2-A2**, respectively. The binding energies (BSSE corrected) for **D2-A1** and **D2-A2** are calculated to be −19.9 and −22.1 kcal/mol, respectively. Hence, substantial stabilization of the donor and acceptor pair by van der Waals interactions due to close proximity between the donor and the acceptor molecules facilitates highly efficient RET. Transition charge densities between the ground and excited states for **D2** and **A2** are calculated within the TDDFT method. The Coulombic coupling matrix elements between **D2** and **A2** are calculated using the transition density cube (TDC) formalism[63] for which grid size of 20 × 20 × 20 was used. For understanding the variation of the Coulomb coupling (V_{DA}) between the donor (**D2**) and the acceptor (**A2**) with increase in separation between them, the distance between **D2** and **A2** (r_{DA}) was increased from an initial 3.5 Å to 100 Å in the parallel π-stacked configuration. Within the TDC method the overlap between the molecular orbital of the donor and acceptor is explicitly considered.

V_{DA} is essentially an electrostatic coupling term between transition charges densities scaled by Coulomb forces, and therefore, V_{DA} has a monotonically decaying behavior.[64,65] For comparison with the experimental data, the percentage of energy transfer between **D2** and **A2** was theoretically estimated as: % of RET at distance $r = V_{DA}(r) \times 100/V_{DA}$ (r = 3.5 Å). Since, the equilibrium intermolecular distance between the monomers is calculated as 3.5 Å (structure shown in Figure 12), maximum RET (100%) must occur at r = 3.5 Å.

Figure 13 shows the variation in the experimental and theoretical percentage of energy transfer for the **D2-A2** pair

dx.doi.org/10.1021/jp409042p | J. Phys. Chem. C 2013, 117, 23178−23189

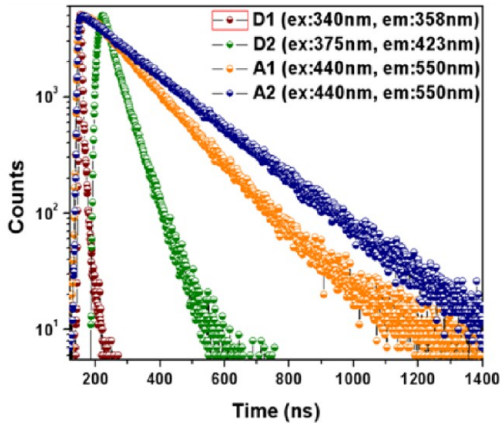

Figure 9. Time correlated single photon count (TCSPC) decay profile of different donors and acceptors recorded for individual samples.

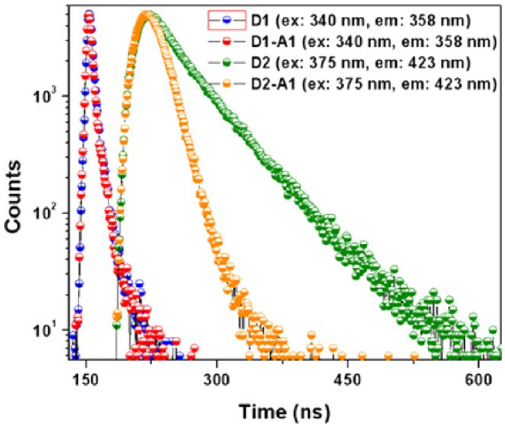

Figure 10. Changes in fluorescence decay profile of different pair of donor−acceptor in chlorobenzene.

Table 2. Lifetimes, Energy Transfer Efficiencies, and Donor's Lifetime for Different Donor−Acceptor Pairs

pair	τ_D (ns)	τ_{DA} (ns)	$E = 1 - (\tau_{DA}/\tau_D)$	% of E
D1-A1	0.181	0.145	0.199	19.9
D1-A2	0.181	0.132	0.2707	27.07
D2-A1	0.21	0.101	0.519	51.9
D2-A2	0.21	0.0995	0.526	52.6

Table 3. Electronic States Involved in Absorption/Emission, Oscillator Strength (f), and Wavelength for Transition (in nm)

molecule	electronic transitions	oscillator strength (f)	λ_{max} (nm)
D1	LUMO → HOMO (100%)	0.90	356.43
D2	LUMO → HOMO (100%)	1.23	391.86
A1	HOMO → LUMO (100%)	0.71	441.76
A2	HOMO → LUMO (100%)	0.73	446.23

with r_{DA}. For both the cases, the data are fitted to a power law of the form: ar^b. For the experimental percentages of RET, a = 3.24 and $b = -3.52 \pm 0.10$, whereas for the theoretical data, a = 350 ± 7.31 and $b = -1.00 \pm 0.01$. Clearly, our results strongly deviate from the well-known r^{-6} behavior expected from a simple dipole−dipole interaction model within the Förster model.[37,38] Higher RET efficiencies for the experimental pair and its faster decay rate with r_{DA} compared to the theoretical

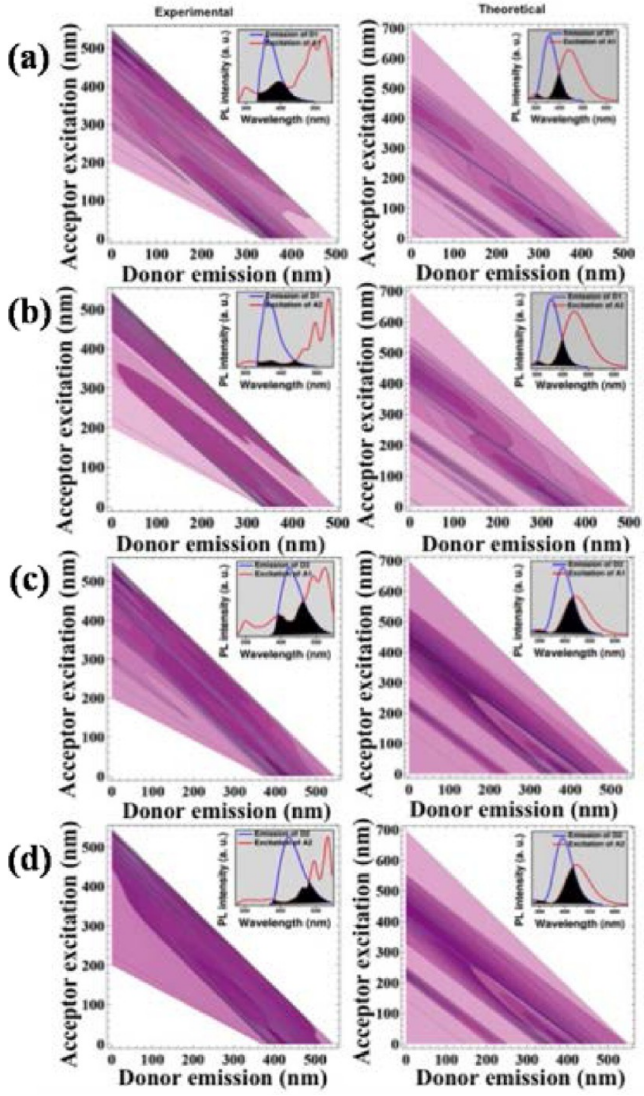

Figure 11. Contour plots and spectral overlap (experimental and theoretical) for the donor emission and acceptor excitations for (a) **D1−A1**, (b) **D1−A2**, (c) **D2−A1**, and (d) **D2−A2** pairs.

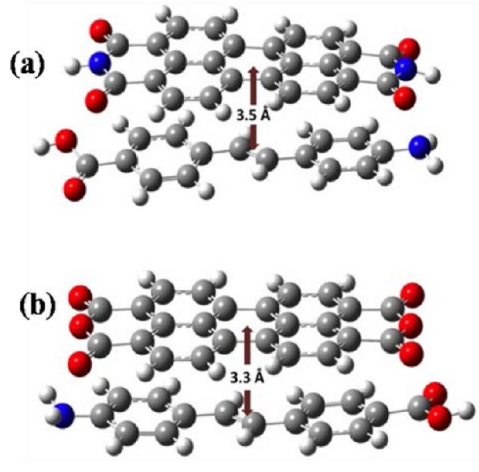

Figure 12. Minimum energy π-stacked structures for **D2-A1** and **D2-A2** dimers.

dx.doi.org/10.1021/jp409042p | J. Phys. Chem. C 2013, 117, 23178−23189

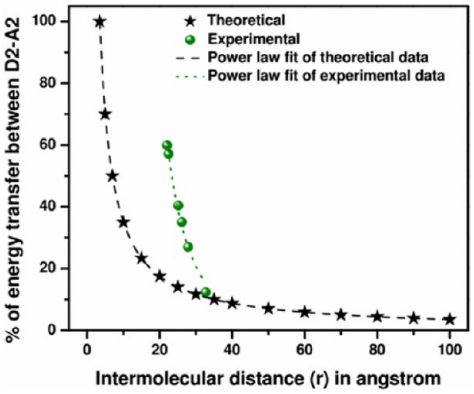

Figure 13. Variation in the percentage of RET as a function intermolecular distance (r) between the donor and acceptor.

Table 4. CIE Coordinates for the Respective White Light Emitting Solutions

donor	donor conc.	acceptor	acceptor conc.	CIE coordinate for white light emission
D1	5.55×10^{-5}	A1	11.1×10^{-5}	0.33, 0.38
D1	5.55×10^{-5}	A2		no white light achieved
D1	5.55×10^{-5}	A3		no white light achieved
D2	2.8×10^{-5}	A1	2.8×10^{-5}	0.30, 0.33
D2	2.8×10^{-5}	A2	2.1×10^{-5}	0.28, 0.31
D2	2.8×10^{-5}	A3	5.04×10^{-5}	0.31, 0.36
D3	3.1×10^{-5}	A1	4.03×10^{-5}	0.30, 0.33
D3	3.1×10^{-5}	A2	4.03×10^{-5}	0.30, 0.35
D3	3.1×10^{-5}	A3	6.2×10^{-5}	0.30, 0.34

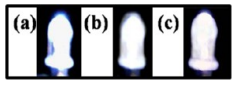

Figure 14. Photographs of commercially available UV-LED coated with white light emitting solutions: **D1-A1** (a), **D2-A1** (b), and **D2-A2** (c).

values may arise due to the possibility of formation of multiple **D2 − A2** pair due to aggregation. Such an aggregation often leads to the rapid energy transfer via a funnel like structure as is known for the photosynthetic proteins.[66] Computational studies match quite well with our experimental results for the measurement of the efficiency of the energy transfer. Both results suggest that **D1-A1** and **D1-A2** are very poor combinations for FRET, whereas **D2-A1** and **D2-A2** are excellent donor−acceptor pairs for FRET indicating the role of **D1** as a poor donor and **D2** as an excellent donor.

CIE Coordinates. The fluorescence resonance energy transfer between donor and acceptor for **D2-A1**, **D2-A2**, **D2-A3**, **D3-A1**, **D3-A2**, and **D3-A3** leads to the generation of a white light emission. Each of these six combinations was able to produce bright white light. The CIE (1931) coordinates for each pair with certain concentration was given in Table 4, and the CIE coordinate figures were given in the Supporting Information as Figure S12. Combination involving the donor **D1**, only the **D1-A1** produces an emission of white light though a very poor energy transfer occurred between the donor and acceptor. This may be due to the combination of two complementary colors. However, the other two combinations involving **D1** like **D1-A2** and **D1-A3**, do not produce any white light emission under similar conditions.

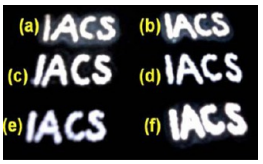

Figure 15. Photograph of writing using the white light emitting solution exposed to a UV lamp of 365 nm: **D1-A1** (a), **D2-A1** (b), **D2-A2** (c), **D2-A3** (d) **D3-A1** (e), and **D3-A2** (f).

These white light emitting solutions can be coated on and also can be used for the coating of LEDs (Figure 14). Photographs of writing by using the white light emitting solution is presented in Figure 15.

CONCLUSION

A series of stilbene moiety containing donors and perylene moiety containing acceptors have been synthesized, purified, characterized, and studied with FRET with an aim to examine the energy transfer efficiency and also to correlate the energy transfer efficiency with the white light emission under suitable conditions. It has been found that good energy transfer efficiency leads to white light emission, and poor energy transfer efficiency suggests no significant emission of white light with one exception. Computational studies also support quite well the experimental results for measuring the efficiency of energy transfer in FRET. The remarkable achievement of this study is that seven out of nine donor−acceptor combinations have produced white light emission, and the energy transfer efficiency can be convincingly correlated with the white light emission except one case out of nine pair. This work should be extended in the future to replace the use of toxic high boiling chlorobenzene solvent by a relatively less toxic high boiling solvent, and in this regard future work is in progress in preferably aqueous medium. These results hold a future promise for the design and construction of new white light emitting materials based on FRET.

ASSOCIATED CONTENT

Supporting Information

Details of the synthesis, NMR spectra, HRMS characterization for **D2**, **D3**, **A1**, **A2**, and **A3**. This material is available free of charge via the Internet at http://pubs.acs.org.

AUTHOR INFORMATION

Corresponding Author

*E-mail: bcab@iacs.res.in and arindamkol1966@gmail.com. Fax: +91-33-2473-2805.

Notes

The authors declare no competing financial interest.

ACKNOWLEDGMENTS

D.K.M. and R.B. would like to acknowledge CSIR, New Delhi, India for financial assistance. A.D. would like to thank DST, CSIR and INSA for partial support.

REFERENCES

(1) D'Andrade, B. W.; Forrest, S. R. White Organic Light-Emitting Devices for Solid-State Lighting. *Adv. Mater.* **2004**, *16*, 1585−1595.

(2) Kamtekar, K. T.; Monkman, A. P.; Bryce, M. R. Recent Advances in White Organic Light-Emitting Materials and Devices (WOLEDs). *Adv. Mater.* **2010**, *22*, 572−582.

(3) Costa, R. D.; Ortí, E.; Bolink, H. J.; Monti, F.; Accorsi, G.; Armaroli, N. Luminescent Ionic Transition-Metal Complexes for Light-Emitting Electrochemical Cells. *Angew. Chem., Int. Ed.* **2012**, *51*, 8178−8121.
(4) Kido, J.; Kimura, M.; Nagai, K. Multilayer White Light-Emitting Organic Electroluminescent Device. *Science* **1995**, *267*, 1332−1334.
(5) Gather, M. C.; Köhnen, A.; Meerholz, M. White Organic Light-Emitting Diodes. *Adv. Mater.* **2011**, *23*, 233−248.
(6) Sun, Y.; Giebink, N. C.; Kanno, H.; Ma, B.; Thompson, M. E.; Forrest, S. R. Management of singlet and triplet excitons for efficient white organic light-emitting devices. *Nature* **2006**, *440*, 908−912.
(7) Vijayakumar, C.; Praveen, V. K.; Ajayaghosh, A. RGB Emission through Controlled Donor Self-Assembly and Modulation of Excitation Energy Transfer: A Novel Strategy to White-Light-Emitting Organogels. *Adv. Mater.* **2009**, *21*, 2059−2063.
(8) Abbel, R.; Weegen, R. v. d.; Pisula, W.; Surin, M.; Leclère, P.; Lazzaroni, R.; Meijer, E. W.; Schenning, A. P. H. J. Multicolour Self-Assembled Fluorene Co-Oligomers: From Molecules to the Solid State via White-Light-Emitting Organogels. *Chem.—Eur. J.* **2009**, *15*, 9737−9746.
(9) Giansante, C.; Raffy, G.; Schäfer, C.; Rahma, H.; Kao, M.-T.; Olive, A. G. L.; Guerzo, A. D. White-Light-Emitting Self-Assembled NanoFibers and Their Evidence by Microspectroscopy of Individual Objects. *J. Am. Chem. Soc.* **2011**, *133*, 316−325.
(10) Shelton, A. H.; Sazanovich, I. V.; Weinstein, J. A.; Ward, M. D. Controllable three-component luminescence from a 1,8-naprhthalimide/Eu(III) complex: white light emission from a single molecule. *Chem. Commun.* **2012**, *48*, 2749−2751.
(11) Liu, Y.; Nishiura, M.; Wang, Y.; Hou, Z. π-Conjugated Aromatic Enynes as a Single-Emitting Component for White Electroluminescence. *J. Am. Chem. Soc.* **2006**, *128*, 5592−5593.
(12) Huynh, H. V.; He, X.; Baumgartner, T. Halochromic generation of white light emission using a single dithienophosphole luminophore. *Chem. Commun.* **2013**, *49*, 4899−4901.
(13) Ki, W.; Li, J.; Eda, G.; Chhowalla, M. Direct white light emission from inorganic−organic hybrid semiconductor bulk materials. *J. Mater. Chem.* **2010**, *20*, 10676−10679.
(14) Huyal, I. O.; Koldemir, U.; Ozel, T.; Demir, H. V.; Tuncel, D. On the origin of high quality white light emission from a hybrid organic/inorganic light emitting diode using azide functionalized polyfluorene. *J. Mater. Chem.* **2008**, *18*, 3568−3574.
(15) Abbel, R.; Grenier, C.; Pouderoijen, M. J.; Stouwdam, J. W.; Leclère, P. E. L. G.; Sijbesma, R. P.; Meijer, E. W.; Schenning, A. P. H. J. White-Light Emitting Hydrogen-Bonded Supramolecular Copolymers Based on π-Conjugated Oligomers. *J. Am. Chem. Soc.* **2009**, *131*, 833−843.
(16) Tu, G.; Mei, C.; Zhou, Q.; Cheng, Y.; Geng, Y.; Wang, L.; Ma, D.; Jing, X.; Wang, F. Highly Efficient Pure-White-Light-Emitting Diodes from a Single Polymer: Polyfluorene with Naphthalimide Moieties. *Adv. Funct. Mater.* **2006**, *16*, 101−106.
(17) Liu, J.; Guo, X.; Bu, L.; Xie, Z.; Cheng, Y.; Geng, Y.; Wang, L.; Jing, X.; Wang, F. White Electroluminescence from a Single-Polymer System with Simultaneous Two-Color Emission: Polyfluorene as Blue Host and 2,1,3-Benzothiadiazole Derivatives as Orange Dopants on the Side Chain. *Adv. Funct. Mater.* **2007**, *17*, 1917−1925.
(18) Shih, H.-M.; Wu, R.-C.; Shih, P.-I.; Wang, C.-L.; Hsu, C.-S. Synthesis of Fluorene-based Hyperbranched Polymers for Solution-Processable Blue, Green, Red, and White Light-Emitting Devices. *J. Polym. Sci., Part A: Polym. Chem.* **2012**, *50*, 696−710.
(19) He, G.; Guo, D.; He, C.; Zhang, X.; Zhao, X.; Duan, C. A Color-Tunable Europium Complex Emitting Three Primary Colors and White Light. *Angew. Chem.* **2009**, *121*, 6248−6251.
(20) Kim, T.-H.; Lee, H. K.; Park, O. O.; Chin, B. D.; Lee, S.-H.; Kim, J. K. White-Light-Emitting Diodes Based on Iridium Complexes via Efficient Energy Transfer from a Conjugated Polymer. *Adv. Funct. Mater.* **2006**, *16*, 611−617.
(21) Ho, C.-L.; Wong, W.-Y.; Wang, Q.; Ma, D.; Wang, L.; Lin, Z. A Multifunctional Iridium-Carbazolyl Orange Phosphor for High-Performance Two-Element WOLED Exploiting Exciton-Managed Fluorescence/Phosphorescence. *Adv. Funct. Mater.* **2008**, *18*, 928−937.
(22) Sykes, D.; Tidmarsh, I. S.; Barbieri, A.; Sazanovich, I. V.; Weinstein, J. A.; Ward, M. D. d-f Energy Transfer in a Series of Ir^{III}/Eu^{III} Dyads: Energy-Transfer Mechanisms and White-Light Emission. *Inorg. Chem.* **2011**, *50*, 11323−11339.
(23) Hou, L.; Duan, L.; Qiao, J.; Zhang, D.; Wang, L.; Cao, Y.; Qiu, Y. Efficient solution-processed phosphor-sensitized single-emitting-layer white organic light-emitting devices: fabrication, characteristics, and transient analysis of energy transfer. *J. Mater. Chem.* **2011**, *21*, 5312−5318.
(24) Lei, Y.; Liao, Q.; Fu, H.; Yao, J. Orange-Blue-Orange Triblock One-Dimensional Heterostructures of Organic Microrods for White-Light Emission. *J. Am. Chem. Soc.* **2010**, *132*, 1742−1743.
(25) Zhao, Y. S.; Fu, H.; Hu, F.; Peng, A.; Yang, W.; Yao, J. Tunable Emission from Binary Organic One-Dimensional Nanomaterials: An Alternative Approach to White-Light Emission. *Adv. Mater.* **2008**, *20*, 79−83.
(26) Sun, H.; Zhang, H.; Zhang, J.; Wei, H.; Ju, J.; Li, M.; Yang, B. White-light emission nanofibers obtained from assembling aqueous single-colored CdTe NCs into a PPV precursor and PVA matrix. *J. Mater. Chem.* **2009**, *19*, 6740−6744.
(27) Ki, W.; Li, J. A Semiconductor Bulk Material That Emits Direct White Light. *J. Am. Chem. Soc.* **2008**, *130*, 8114−8115.
(28) Rao, K. V.; Datta, K. K. R.; Eswaramoorthy, M.; George, S. J. Highly Pure Solid-State White-Light Emission from Solution-Processable Soft-Hybrids. *Adv. Mater.* **2013**, *25*, 1713−1718.
(29) Vijayakumar, C.; Sugiyasu, K.; Takeuchi, M. Oligofluorene-based electrophoretic nanoparticles in aqueous medium as a donor scaffold for fluorescence resonance energy transfer and white-light emission. *Chem. Sci.* **2011**, *2*, 291−294.
(30) Roushan, M.; Zhang, X.; Li, J. Solution-Processable White-Light-Emitting Hybrid Semiconductor Bulk Materials with High Photoluminescence Quantum Efficiency. *Angew. Chem., Int. Ed.* **2012**, *51*, 436−439.
(31) Maiti, D. K.; Banerjee, A. A peptide based two component white light emitting system. *Chem. Commun.* **2013**, *49*, 6909−6911.
(32) Fang, X.; Roushan, M.; Zhang, R.; Peng, J.; Zeng, H.; Li, J. Tuning and Enhancing White Light Emission of II−VI Based Inorganic−Organic Hybrid Semiconductors as Single-Phased Phosphors. *Chem. Mater.* **2012**, *24*, 1710−1717.
(33) Babu, S. S.; Aimi, J.; Ozawa, H.; Shirahata, N.; Saeki, A.; Seki, S.; Ajayaghosh, A.; Möhwald, H.; Nakanishi, T. Solvent-Free Luminescent Organic Liquids. *Angew. Chem., Int. Ed.* **2012**, *51*, 3391−3395.
(34) Liu, S.; Li, F.; Diao, Q.; Ma, Y. Aggregation-induced enhanced emission materials for efficient white organic light-emitting devices. *Org. Electron.* **2010**, *11*, 613−617.
(35) Park, S.; Kwon, J. E.; Kim, S. H.; Seo, J.; Chung, K.; Park, S.-Y.; Jang, D.-J.; Medina, B. M.; Gierschner, J.; Park, S. Y. A White-Light-Emitting Molecule: Frustrated Energy Transfer between Constituent Emitting Centers. *J. Am. Chem. Soc.* **2009**, *131*, 14043−14049.
(36) Wang, R.; Peng, J.; Qiu, F.; Yang, Y. Enhanced white-light emission from multiple fluorophores encapsulated in a single layer of diblock copolymer micelles. *Chem. Commun.* **2011**, *47*, 2787−2789.
(37) Förster, T. Transfer Mechanisms of Electronic Excitation. *Discuss. Faraday Soc.* **1959**, *27*, 7−17.
(38) Lakowicz, J. R. *Principles of Fluorescence Spectroscopy*, 2nd ed.; Kluwer/Plenum: New York, 1999.
(39) Stryer, L. Fluorescence Energy Transfer as a Spectroscopic Ruler. *Annu. Rev. Biochem.* **1978**, *47*, 819−846.
(40) Sahoo, H. Förster resonance energy transfer − A spectroscopic nanoruler: Principle and applications. *J. Photochem. Photobiol. C* **2011**, *12*, 20−30.
(41) Yuan, L.; Lin, W.; Zheng, K.; Zhu, S. FRET-Based Small-Molecule Fluorescent Probes: Rational Design and Bioimaging Applications. *Acc. Chem. Res.* **2013**, *46*, 1462−1473.
(42) Lu, S.; Wang, Y.; Huang, H.; Pan, Y.; Chaney, E. J.; Boppart, S. A.; Ozer, H.; Strongin, A. Y.; Wang, Y. Quantitative FRET Imaging to

Visualize the Invasiveness of Live Breast Cancer Cells. *PLOS One* **2013**, *8*, e58569(1−9).
(43) Yuan, L.; Lin, W.; Chen, B.; Xie, Y. Development of FRET-Based Ratiometric Fluorescent Cu^{2+} Chemodosimeters and the Applications for Living Cell Imaging. *Org. Lett.* **2012**, *14*, 432−435.
(44) Suzuki, M.; Husimi, Y.; Komatsu, H.; Suzuki, K.; Douglas, K. T. Quantum Dot FRET Biosensors that Respond to pH, to Proteolytic or Nucleolytic Cleavage, to DNA Synthesis, or to a Multiplexing Combination. *J. Am. Chem. Soc.* **2008**, *130*, 5720−5725.
(45) Huebsch, N. D.; Mooney, D. J. Fluorescent Resonance Energy Transfer: A Tool for Probing Molecular Cell-Biomaterial Interactions in Three Dimensions. *Biomaterials* **2007**, *28*, 2424−2437.
(46) Sahoo, H.; Nau, W. M. Phosphorylation-Induced Conformational Changes in Short Peptides Probed by Fluorescence Resonance Energy Transfer in the 10 Å Domain. *ChemBioChem* **2007**, *8*, 567−573.
(47) Sahoo, H.; Roccatano, D.; Hennig, A.; Nau, W. M. A 10-Å Spectroscopic Ruler Applied to Short Polyprolines. *J. Am. Chem. Soc.* **2007**, *129*, 9762−9772.
(48) Ward, M. D. Photo-induced electron and energy transfer in non-covalently bonded supramolecular assemblies. *Chem. Soc. Rev.* **1997**, *26*, 365−375.
(49) Praveen, V. K.; George, S. J.; Varghese, R.; Vijayakumar, C.; Ajayaghosh, A. Self-Assembled π-Nanotapes as Donor Scaffolds for Selective and Thermally Gated Fluorescence Resonance Energy Transfer (FRET). *J. Am. Chem. Soc.* **2006**, *128*, 7542−7550.
(50) Guerzo, A. D.; Olive, A. G. L.; Reichwagen, J.; Hopf, H.; Desvergne, J.-P. Energy Transfer in Self-Assembled [n]-Acene Fibers Involving ≥100 Donors Per Acceptor. *J. Am. Chem. Soc.* **2005**, *127*, 17984−17985.
(51) Hippius, C.; van Stokkum, I. H. M.; Gsänger, M.; Groeneveld, M. M.; Williams, R. M.; Würthner, F. Sequential FRET Processes in Calix[4]arene-Linked Orange-Red-Green Perylene Bisimide Dye Zigzag Arrays. *J. Phys. Chem. C* **2008**, *112*, 2476−2486.
(52) Samanta, S. K.; Bhattacharya, S. Wide-Range Light-Harvesting Donor−Acceptor Assemblies through Specific Intergelator Interactions via Self-Assembly. *Chem.—Eur. J.* **2012**, *18*, 15875−15885.
(53) Maiti, D. K.; Banerjee, A. A Synthetic Amino Acid Residue Containing A New Oligopeptide-Based Photosensitive Fluorescent. Organogel. *Chem. Asian J.* **2013**, *8*, 113−120.
(54) Würthner, F.; Stepanenko, V.; Chen, Z.; Saha-Möller, C. R.; Kocher, N.; Stalke, D. Preparation and Characterization of Regioisomerically Pure 1,7-Disubstituted Perylene Bisimide Dyes. *J. Org. Chem.* **2004**, *69*, 7933−7939.
(55) Dubey, R. K.; Niemi, M.; Kaunisto, K.; Efimov, A.; Tkachenko, N. V.; Lemmetyinen, H. Direct Evidence of Significantly Different Chemical Behavior and Excited-State Dynamics of 1,7- and 1,6-Regioisomers of Pyrrolidinyl-Substituted Perylene Diimide. *Chem.—Eur. J.* **2013**, *19*, 6791−6806.
(56) Frisch, M. J.; Trucks, G. W.; Schlegel, H. B.; Scuseria, G. E.; Robb, M. A.; Cheeseman, J. R.; Scalmani, G.; Barone, V.; Mennucci, B.; Petersson, G. A.; Nakatsuji, H.; Caricato, M.; Li, X.; Hratchian, H. P.; Izmaylov, A. F.; Bloino, J.; Zheng, G.; Sonnenberg, J. L.; Hada, M.; Ehara, M.; Toyota, K.; Fukuda, R.; Hasegawa, J.; Ishida, M.; Nakajima, T.; Honda, Y.; Kitao, O.; Nakai, H.; Vreven, T.; Montgomery, Jr., J. A.; Peralta, J. E.; Ogliaro, F.; Bearpark, M.; Heyd, J. J.; Brothers, E.; Kudin, K. N.; Staroverov, V. N.; Kobayashi, R.; Normand, J.; Raghavachari, K.; Rendell, A.; Burant, J. C.; Iyengar, S. S.; Tomasi, J.; Cossi, M.; Rega, N.; Millam, J. M.; Klene, M.; Knox, J. E.; Cross, J. B.; Bakken, V.; Adamo, C.; Jaramillo, J.; Gomperts, R.; Stratmann, R. E.; Yazyev, O.; Austin, A. J.; Cammi, R.; Pomelli, C.; Ochterski, J. W.; Martin, R. L.; Morokuma, K.; Zakrzewski, V. G.; Voth, G. A.; Salvador, P.; Dannenberg, J. J.; Dapprich, S.; Daniels, A. D.; Farkas, Ö.; Foresman, J. B.; Ortiz, J. V.; Cioslowski, J.; Fox, D. J. *Gaussian 09*, revision A.1; Gaussian, Inc.: Wallingford, CT, 2009.
(57) Zhao, Y.; Truhlar, D. G. The M06 suite of density functionals for main group thermochemistry, thermochemical kinetics, noncovalent interactions, excited states, and transition elements: two new functionals and systematic testing of four M06-class functionals and 12 other functionals. *Theor. Chem. Acc.* **2008**, *120*, 215−241.
(58) Jissy, A. K.; Datta, A. Effect of External Electric Field on H-Bonding and π-Stacking Interactions in Guanine Aggregates. *ChemPhysChem* **2012**, *13*, 4163−4172.
(59) Jose, D.; Datta, A. Role of Multicentered Bonding in Controlling Magnetic Interactions in π-Stacked Bis-dithiazolyl Radical. *Cryst. Growth Design* **2011**, *11*, 3137−3140.
(60) Zhao, G.-J.; Liu, J.-Y.; Zhou, L.-C.; Han, K.-L. Site-Selective Photoinduced Electron Transfer from Alcoholic Solvents to the Chromophore Facilitated by Hydrogen Bonding: A New Fluorescence Quenching Mechanism. *J. Phys. Chem. B* **2007**, *111*, 8940−8945.
(61) Zhao, G.-J.; Han, K.-L. Hydrogen Bonding in the Electronic Excited State. *Acc. Chem. Res.* **2012**, *45*, 404−413.
(62) Zhang, M.-X.; Zhao, G.-J. Modification of n-Type Organic Semiconductor Performance of Perylene Diimides by Substitution in Different Positions: Two-Dimensional π-Stacking and Hydrogen Bonding. *ChemSusChem* **2012**, *5*, 879−887.
(63) Kruger, B. P.; Scholes, G. D.; Fleming, G. R. Calculation of Couplings and Energy-Transfer Pathways between the Pigments of LH2 by the ab Initio Transition Density Cube Method. *J. Phys. Chem. B* **1998**, *102*, 5378−5386.
(64) Sissa, C.; Manna, A. K.; Terenziani, F.; Painelli, A.; Pati, S. K. Beyond the Fö rster formulation for resonance energy transfer: the role of dark states. *Phys. Chem. Chem. Phys.* **2011**, *13*, 12734−12744.
(65) Sissa, C.; Terenziani, F.; Painelli, A.; Manna, A. K.; Pati, S. K. Resonance energy transfer between polar charge-transfer dyes: A focus on the limits of the dipolar approximation. *Chem. Phys.* **2012**, *404*, 9−15.
(66) Ritz, T.; Damjanović, A.; Schulten, K. The Quantum Physics of Photosynthesis. *ChemPhysChem* **2002**, *3*, 243−248.